Supplemental Table 1. Sequences for primers used for qPCR

Gene	Forward Primer	Reverse Primer
Sbds	AGCGGGCCCACATGCGATT	CTCTGAAGCAGCCTGGGTCGA
Spp1	CCTGGCTGAATTCTGAGGGACT	GCTTCTGAGATGGGTCAGGCA
Pparg	TCATGACCAGGGAGTTCCTC	CAGGTTGTCTTGGATGTCCTC
Fabp4	ATAACCCTAGATGGCGGGGC	GCCTCTTCCTTTGGCTCATGC
Adipoq	GATGGCAGAGATGGCACTCCT	GGCCCTTCAGCTCCTGTCATT
Igfbp2	ACCCCTTGCCAGCAGGAGTTGGA	TCCCTGGATGGGCTTCCCGGT
Igfbp3	GAGGCGTCCACATCCCAAAC	CCCTTGGTGTCGTAGCCTGG
Igf1r	GATCGCGATTTCTGCGCCAA	GCCTTCGCAGGGGATACAGT
Raf1	GCTAATTGACATTGCCCGACA	TTCAACCTGCTGAGAACCAC
Fos	GAAGACCGTGTCAGGAGGCA	CTCCTCCGATTCCGGCACTT
Rpl3l	CATTTGACCTCTGGTGCCTGG	CGAGGGGCAGAGAACTTCCG
Rsl24d1	AGCTCACGGTGGACAACTCA	ATTTGGCCTGGCGCTTCTGT
Trp53	TCCGAAGACTGGATGACTGCCA	CATCCTGGGGCAGCAACAGA
Ddit4	GAGCCTGGAGAGCTCGGAC	AGGGACACCCCATCCAGGTAT
Ercc5	CTAACGGGAAACAAAGGCCC	TCCCATGGCTATCTCGGACT
Nupr1	GATCAGTACAGCCTGGCCCAT	AGGGCGGTTGGTATTGGCA
Plk2	TGGAACGTCCGCAGTGGAAA	ACAGTCAGCTTCCGGCATGT

Supplemental Table 2. Antibodies used for flow cytometry and immunohistochemistry analysis.

Antibodies for Flow Cytometry			
Target	**Fluorophore**	**Company**	**Clone**
CD117(c-Kit)	APC-eFlour780	eBioscience	ACK2
CD11b	PE-Cy7	eBioscience	M1/70
CD150	PerCP-eFluor710	eBioscience	mShad150
CD31	FITC	BioLegend	390
CD3e	PE	eBioscience	145-2C11
CD4	PE-Cy7	BD Pharmingen	RM4-5
CD45	APC	eBioscience	30-F11
CD45R(B220)	PE-Cy7	eBioscience	RA3-6B2
CD48	APC	eBioscience	HM48-1
CD51	PE	BioLegend	RMV-7
CD8a	PE-Cy7	eBioscience	53-6.7
F4/80	AlexiaFluor647	BioLegend	BM8
Ly6A/E(Sca-1)	PE	BD Pharmingen	D7
Ly6G	FITC	BioLegend	1A8
Ly6G(Gr1)	PE-Cy7	eBioscience	RB6-8C5
TER-119	PE-Cy7	eBioscience	TER-119
TER-119	AlexiaFluor647	BioLegend	TER-119
Antibodies for Immunohistochemistry			
Target	**Company**	**Catalog**	
Active Caspase-3	R&D Systems	AF835	
PPAR-γ	Invitrogen	MA5-14889	
SDF1(CXCL12)	Invitrogen	PA5-114344	

Supplemental Table 3. Gene set enrichment analysis results show dysregulated signaling pathways in the bone marrow stromal cells from *Mx1^{Cre}Sbds^{Exc}* mice compared to *Sbds$^{l/l}$* controls (p<0.05, FDR<0.25)

Gene set	NES	*p* Value	FDR
Enriched in *Mx1^{Cre}Sbds$^{l/l}$*			
HALLMARK_HEME_METABOLISM	6.68	0.000	0.000
NABA_CORE_MATRISOME	5.49	0.000	0.000
HALLMARK_EPITHELIAL_MESENCHYMAL_TRANSITION	5.32	0.000	0.000
NABA_MATRISOME_ASSOCIATED	5.01	0.000	0.000
NABA_ECM_GLYCOPROTEINS	4.52	0.000	0.000
HALLMARK_MYOGENESIS	3.96	0.000	0.000
KEGG_ECM_RECEPTOR_INTERACTION	3.58	0.000	0.000
PID_INTEGRIN1_PATHWAY	3.51	0.000	0.000
NABA_SECRETED_FACTORS	3.42	0.000	0.000
NABA_ECM_REGULATORS	3.31	0.000	0.000
NABA_PROTEOGLYCANS	2.95	0.000	0.000
REACTOME_COLLAGEN_FORMATION	2.87	0.000	0.000
REACTOME_EXTRACELLULAR_MATRIX_ORGANIZATION	2.76	0.000	0.000
NABA_COLLAGENS	2.71	0.000	0.000
KEGG_FOCAL_ADHESION	2.71	0.000	0.000
REACTOME_NETRIN1_SIGNALING	2.70	0.000	0.000
KEGG_BASAL_CELL_CARCINOMA	2.66	0.000	0.001
REACTOME_AMINO_ACID_TRANSPORT_ACROSS_THE_PLASMA_MEMBRANE	2.64	0.000	0.001
NABA_BASEMENT_MEMBRANES	2.61	0.000	0.001
PID_INTEGRIN3_PATHWAY	2.59	0.000	0.001
REACTOME_GLYCOSAMINOGLYCAN_METABOLISM	2.57	0.000	0.002
HALLMARK_KRAS_SIGNALING_UP	2.57	0.000	0.002
HALLMARK_APICAL_JUNCTION	2.54	0.000	0.002
HALLMARK_UV_RESPONSE_DN	2.54	0.000	0.002
PID_AVB3_INTEGRIN_PATHWAY	2.50	0.000	0.002
REACTOME_NCAM1_INTERACTIONS	2.47	0.000	0.002
REACTOME_INTEGRIN_CELL_SURFACE_INTERACTIONS	2.42	0.000	0.004
REACTOME_TRANSPORT_OF_INORGANIC_CATIONS_ANIONS_AND_AMINO_ACIDS_OLIGOPEPTIDES	2.40	0.000	0.004
PID_WNT_SIGNALING_PATHWAY	2.38	0.000	0.005
BIOCARTA_P53HYPOXIA_PATHWAY	2.38	0.000	0.005
KEGG_CELL_ADHESION_MOLECULES_CAMS	2.37	0.000	0.005
HALLMARK_ESTROGEN_RESPONSE_EARLY	2.34	0.004	0.006
REACTOME_AXON_GUIDANCE	2.29	0.002	0.008
REACTOME_AMINO_ACID_AND_OLIGOPEPTIDE_SLC_TRANSPORTERS	2.28	0.000	0.008
PID_INTEGRIN_A9B1_PATHWAY	2.26	0.002	0.009
HALLMARK_APICAL_SURFACE	2.26	0.002	0.009
HALLMARK_ADIPOGENESIS	2.23	0.000	0.010
BIOCARTA_COMP_PATHWAY	2.23	0.002	0.010
REACTOME_HS_GAG_BIOSYNTHESIS	2.22	0.000	0.011
BIOCARTA_ALK_PATHWAY	2.21	0.002	0.012
PID_SYNDECAN_4_PATHWAY	2.20	0.002	0.012
REACTOME_DEVELOPMENTAL_BIOLOGY	2.19	0.002	0.012

REACTOME_GENERATION_OF_SECOND_MESSENGER_MOLECULES	2.16	0.006	0.015
HALLMARK_ANGIOGENESIS	2.16	0.002	0.014
HALLMARK_XENOBIOTIC_METABOLISM	2.16	0.002	0.014
REACTOME_3_UTR_MEDIATED_TRANSLATIONAL_REGULATION	2.15	0.000	0.015
REACTOME_CLASS_B_2_SECRETIN_FAMILY_RECEPTORS	2.11	0.000	0.019
KEGG_AXON_GUIDANCE	2.10	0.002	0.020
REACTOME_HEPARAN_SULFATE_HEPARIN_HS_GAG_METABOLISM	2.06	0.008	0.023
REACTOME_COSTIMULATION_BY_THE_CD28_FAMILY	2.05	0.000	0.024
REACTOME_CELL_CELL_JUNCTION_ORGANIZATION	2.04	0.006	0.026
BIOCARTA_CTLA4_PATHWAY	2.04	0.006	0.027
REACTOME_CELL_JUNCTION_ORGANIZATION	2.03	0.012	0.028
REACTOME_MYOGENESIS	2.01	0.002	0.029
BIOCARTA_NFAT_PATHWAY	2.01	0.002	0.029
KEGG_ARRHYTHMOGENIC_RIGHT_VENTRICULAR_CARDIOMYOPATHY_ARVC	2.00	0.006	0.031
KEGG_HEMATOPOIETIC_CELL_LINEAGE	2.00	0.006	0.030
HALLMARK_HYPOXIA	2.00	0.002	0.030
REACTOME_NCAM_SIGNALING_FOR_NEURITE_OUT_GROWTH	1.99	0.000	0.031
KEGG_T_CELL_RECEPTOR_SIGNALING_PATHWAY	1.97	0.002	0.033
PID_NFAT_TFPATHWAY	1.97	0.010	0.034
NABA_ECM_AFFILIATED	1.96	0.006	0.035
BIOCARTA_CTCF_PATHWAY	1.96	0.008	0.035
BIOCARTA_CSK_PATHWAY	1.94	0.009	0.038
REACTOME_FORMATION_OF_THE_TERNARY_COMPLEX_AND_SUBSEQUENTLY_THE_43S_COMPLEX	1.94	0.004	0.038
KEGG_DILATED_CARDIOMYOPATHY	1.92	0.008	0.043
REACTOME_PI3K_EVENTS_IN_ERBB2_SIGNALING	1.91	0.012	0.043
HALLMARK_COMPLEMENT	1.91	0.010	0.043
REACTOME_PI_3K_CASCADE	1.89	0.010	0.047
REACTOME_KERATAN_SULFATE_BIOSYNTHESIS	1.89	0.010	0.048
HALLMARK_IL2_STAT5_SIGNALING	1.89	0.010	0.048
REACTOME_KERATAN_SULFATE_KERATIN_METABOLISM	1.88	0.012	0.049
PID_SYNDECAN_1_PATHWAY	1.86	0.012	0.054
KEGG_COMPLEMENT_AND_COAGULATION_CASCADES	1.83	0.016	0.061
REACTOME_INTERACTION_BETWEEN_L1_AND_ANKYRINS	1.83	0.012	0.062
REACTOME_TRANSMEMBRANE_TRANSPORT_OF_SMALL_MOLECULES	1.82	0.019	0.064
KEGG_PRIMARY_IMMUNODEFICIENCY	1.80	0.010	0.068
KEGG_PPAR_SIGNALING_PATHWAY	1.79	0.007	0.072
REACTOME_A_TETRASACCHARIDE_LINKER_SEQUENCE_IS_REQUIRED_FOR_GAG_SYNTHESIS	1.78	0.008	0.074
REACTOME_SIGNALING_BY_PDGF	1.77	0.012	0.079
KEGG_CARDIAC_MUSCLE_CONTRACTION	1.76	0.012	0.083
REACTOME_GLUTATHIONE_CONJUGATION	1.75	0.012	0.083
REACTOME_BASIGIN_INTERACTIONS	1.75	0.018	0.085
PID_BMP_PATHWAY	1.75	0.025	0.085
REACTOME_CHONDROITIN_SULFATE_DERMATAN_SULFATE_METABOLISM	1.73	0.016	0.091
REACTOME_CELL_CELL_COMMUNICATION	1.73	0.029	0.091
KEGG_ADHERENS_JUNCTION	1.72	0.008	0.093
KEGG_CYTOKINE_CYTOKINE_RECEPTOR_INTERACTION	1.72	0.022	0.093

PID_FGF_PATHWAY	1.71	0.036	0.097
HALLMARK_COAGULATION	1.70	0.019	0.099
REACTOME_SLC_MEDIATED_TRANSMEMBRANE_TRANSPORT	1.69	0.037	0.101
PID_HNF3A_PATHWAY	1.69	0.033	0.101
PID_INTEGRIN5_PATHWAY	1.69	0.030	0.103
REACTOME_PHOSPHOLIPASE_C_MEDIATED_CASCADE	1.68	0.032	0.104
KEGG_AMINOACYL_TRNA_BIOSYNTHESIS	1.67	0.029	0.107
KEGG_CALCIUM_SIGNALING_PATHWAY	1.67	0.030	0.108
WNT_SIGNALING	1.66	0.033	0.115
BIOCARTA_NO2IL12_PATHWAY	1.64	0.039	0.121
PID_DELTA_NP63_PATHWAY	1.64	0.027	0.124
BIOCARTA_STATHMIN_PATHWAY	1.63	0.033	0.124
REACTOME_DEGRADATION_OF_THE_EXTRACELLULAR_MATRIX	1.63	0.033	0.125
KEGG_HYPERTROPHIC_CARDIOMYOPATHY_HCM	1.62	0.036	0.127
HALLMARK_P53_PATHWAY	1.62	0.039	0.126
PID_EPHRINB_REV_PATHWAY	1.62	0.040	0.126
HALLMARK_KRAS_SIGNALING_DN	1.62	0.033	0.126
PID_TAP63_PATHWAY	1.61	0.050	0.129
REACTOME_DOWNSTREAM_SIGNALING_OF_ACTIVATED_FGFR	1.61	0.044	0.129
BIOCARTA_TOB1_PATHWAY	1.61	0.036	0.128
REACTOME_CIRCADIAN_CLOCK	1.60	0.032	0.130
REACTOME_LIPOPROTEIN_METABOLISM	1.60	0.035	0.132
KEGG_PORPHYRIN_AND_CHLOROPHYLL_METABOLISM	1.59	0.040	0.136
REACTOME_PI3K_EVENTS_IN_ERBB4_SIGNALING	1.56	0.046	0.151
REACTOME_TCR_SIGNALING	1.52	0.046	0.172
Enriched in *Sbds*$^{l/l}$ controls			
REACTOME_DNA_REPLICATION	-4.20	0.000	0.000
REACTOME_CELL_CYCLE_MITOTIC	-3.87	0.000	0.000
HALLMARK_E2F_TARGETS	-3.85	0.000	0.000
PID_IL8_CXCR2_PATHWAY	-3.77	0.000	0.000
REACTOME_MITOTIC_M_M_G1_PHASES	-3.76	0.000	0.000
REACTOME_DNA_STRAND_ELONGATION	-3.71	0.000	0.000
REACTOME_MRNA_PROCESSING	-3.56	0.000	0.000
REACTOME_MITOTIC_PROMETAPHASE	-3.56	0.000	0.000
REACTOME_MRNA_SPLICING	-3.53	0.000	0.000
REACTOME_PROCESSING_OF_CAPPED_INTRON_CONTAINING_PRE_MRNA	-3.48	0.000	0.000
HALLMARK_G2M_CHECKPOINT	-3.41	0.000	0.000
REACTOME_CELL_CYCLE	-3.28	0.000	0.000
HALLMARK_MYC_TARGETS_V1	-3.26	0.000	0.000
REACTOME_PLATELET_ACTIVATION_SIGNALING_AND_AGGREGATION	-3.20	0.000	0.000
REACTOME_METABOLISM_OF_RNA	-3.17	0.000	0.000
KEGG_DNA_REPLICATION	-3.12	0.000	0.000
HALLMARK_DNA_REPAIR	-3.12	0.000	0.000
REACTOME_TRANSCRIPTION	-3.06	0.000	0.000
BIOCARTA_HIVNEF_PATHWAY	-3.03	0.000	0.000
KEGG_SPLICEOSOME	-3.01	0.000	0.000

HALLMARK_TNFA_SIGNALING_VIA_NFKB	-2.97	0.000	0.000
REACTOME_HEMOSTASIS	-2.93	0.000	0.000
REACTOME_CYTOKINE_SIGNALING_IN_IMMUNE_SYSTEM	-2.92	0.000	0.000
REACTOME_EXTENSION_OF_TELOMERES	-2.91	0.000	0.000
KEGG_LEUKOCYTE_TRANSENDOTHELIAL_MIGRATION	-2.90	0.000	0.000
REACTOME_SRP_DEPENDENT_COTRANSLATIONAL_PROTEIN_TARGETING_TO_MEMBRANE	-2.89	0.000	0.000
HALLMARK_INFLAMMATORY_RESPONSE	-2.82	0.000	0.000
REACTOME_INFLUENZA_VIRAL_RNA_TRANSCRIPTION_AND_REPLICATION	-2.80	0.000	0.000
PID_PDGFRB_PATHWAY	-2.79	0.000	0.000
HALLMARK_MITOTIC_SPINDLE	-2.78	0.000	0.000
REACTOME_LAGGING_STRAND_SYNTHESIS	-2.78	0.000	0.000
REACTOME_INFLUENZA_LIFE_CYCLE	-2.78	0.000	0.000
REACTOME_RNA_POL_II_TRANSCRIPTION	-2.77	0.000	0.000
REACTOME_METABOLISM_OF_MRNA	-2.76	0.000	0.000
KEGG_FC_GAMMA_R_MEDIATED_PHAGOCYTOSIS	-2.73	0.000	0.001
KEGG_PHOSPHATIDYLINOSITOL_SIGNALING_SYSTEM	-2.73	0.000	0.001
PID_IL8_CXCR1_PATHWAY	-2.71	0.000	0.001
KEGG_CHEMOKINE_SIGNALING_PATHWAY	-2.71	0.000	0.001
KEGG_LEISHMANIA_INFECTION	-2.69	0.000	0.001
KEGG_INOSITOL_PHOSPHATE_METABOLISM	-2.67	0.000	0.001
BIOCARTA_RHO_PATHWAY	-2.67	0.000	0.001
BIOCARTA_MAPK_PATHWAY	-2.62	0.000	0.001
REACTOME_GPVI_MEDIATED_ACTIVATION_CASCADE	-2.60	0.000	0.001
KEGG_RIBOSOME	-2.58	0.002	0.001
HALLMARK_OXIDATIVE_PHOSPHORYLATION	-2.58	0.000	0.001
REACTOME_S_PHASE	-2.58	0.000	0.001
REACTOME_RNA_POL_II_PRE_TRANSCRIPTION_EVENTS	-2.54	0.000	0.002
REACTOME_TRANSCRIPTION_COUPLED_NER_TC_NER	-2.53	0.000	0.002
REACTOME_MRNA_SPLICING_MINOR_PATHWAY	-2.52	0.000	0.002
PID_TXA2PATHWAY	-2.50	0.002	0.002
PID_MAPK_TRK_PATHWAY	-2.50	0.000	0.002
REACTOME_INNATE_IMMUNE_SYSTEM	-2.50	0.002	0.002
KEGG_ACUTE_MYELOID_LEUKEMIA	-2.49	0.000	0.002
REACTOME_NONSENSE_MEDIATED_DECAY_ENHANCED_BY_THE_EXON_JUNCTION_COMPLEX	-2.48	0.000	0.002
REACTOME_ACTIVATION_OF_THE_PRE_REPLICATIVE_COMPLEX	-2.48	0.000	0.002
KEGG_NEUROTROPHIN_SIGNALING_PATHWAY	-2.47	0.000	0.003
KEGG_APOPTOSIS	-2.47	0.000	0.003
ST_B_CELL_ANTIGEN_RECEPTOR	-2.46	0.000	0.003
KEGG_B_CELL_RECEPTOR_SIGNALING_PATHWAY	-2.45	0.000	0.003
REACTOME_INTERFERON_SIGNALING	-2.45	0.000	0.003
REACTOME_LATENT_INFECTION_OF_HOMO_SAPIENS_WITH_MYCOBACTERIUM_TUBERCULOSIS	-2.44	0.000	0.003
REACTOME_DNA_REPAIR	-2.44	0.000	0.003
PID_CXCR4_PATHWAY	-2.44	0.000	0.003
KEGG_PANCREATIC_CANCER	-2.44	0.000	0.003
REACTOME_PEROXISOMAL_LIPID_METABOLISM	-2.43	0.000	0.003
HALLMARK_INTERFERON_GAMMA_RESPONSE	-2.43	0.000	0.003

KEGG_NATURAL_KILLER_CELL_MEDIATED_CYTOTOXICITY	-2.42	0.002	0.003
BIOCARTA_KERATINOCYTE_PATHWAY	-2.42	0.000	0.003
REACTOME_PEPTIDE_CHAIN_ELONGATION	-2.41	0.004	0.004
PID_AVB3_OPN_PATHWAY	-2.41	0.002	0.004
REACTOME_PROCESSIVE_SYNTHESIS_ON_THE_LAGGING_STRAND	-2.40	0.000	0.004
KEGG_PATHOGENIC_ESCHERICHIA_COLI_INFECTION	-2.40	0.000	0.004
BIOCARTA_CERAMIDE_PATHWAY	-2.40	0.002	0.004
REACTOME_SIGNALLING_BY_NGF	-2.39	0.002	0.004
REACTOME_P75_NTR_RECEPTOR_MEDIATED_SIGNALLING	-2.39	0.000	0.004
REACTOME_SYNTHESIS_OF_DNA	-2.39	0.000	0.004
PID_ERBB1_DOWNSTREAM_PATHWAY	-2.38	0.000	0.004
REACTOME_METABOLISM_OF_PROTEINS	-2.37	0.000	0.004
REACTOME_FORMATION_OF_RNA_POL_II_ELONGATION_COMPLEX_	-2.36	0.000	0.005
PID_RAC1_PATHWAY	-2.35	0.000	0.005
HALLMARK_IL6_JAK_STAT3_SIGNALING	-2.35	0.002	0.005
PID_ILK_PATHWAY	-2.35	0.000	0.005
REACTOME_CLEAVAGE_OF_GROWING_TRANSCRIPT_IN_THE_TERMINATION_REGION_	-2.34	0.000	0.005
REACTOME_LATE_PHASE_OF_HIV_LIFE_CYCLE	-2.33	0.000	0.005
PID_HDAC_CLASSI_PATHWAY	-2.31	0.000	0.006
REACTOME_HIV_INFECTION	-2.31	0.002	0.006
REACTOME_INTERFERON_ALPHA_BETA_SIGNALING	-2.30	0.000	0.006
REACTOME_CHROMOSOME_MAINTENANCE	-2.29	0.002	0.006
BIOCARTA_CDMAC_PATHWAY	-2.29	0.002	0.007
REACTOME_RNA_POL_I_TRANSCRIPTION	-2.29	0.000	0.007
KEGG_DRUG_METABOLISM_OTHER_ENZYMES	-2.28	0.006	0.007
REACTOME_SIGNALING_BY_ILS	-2.28	0.002	0.007
KEGG_STARCH_AND_SUCROSE_METABOLISM	-2.27	0.000	0.007
BIOCARTA_TPO_PATHWAY	-2.26	0.000	0.007
REACTOME_GLUCOSE_METABOLISM	-2.25	0.002	0.008
PID_THROMBIN_PAR1_PATHWAY	-2.24	0.000	0.008
KEGG_FC_EPSILON_RI_SIGNALING_PATHWAY	-2.24	0.002	0.008
REACTOME_G2_M_CHECKPOINTS	-2.23	0.000	0.009
REACTOME_NUCLEOTIDE_EXCISION_REPAIR	-2.23	0.000	0.009
REACTOME_SIGNALLING_TO_RAS	-2.22	0.004	0.009
REACTOME_SEMA4D_IN_SEMAPHORIN_SIGNALING	-2.21	0.000	0.009
REACTOME_SEMA4D_INDUCED_CELL_MIGRATION_AND_GROWTH_CONE_COLLAPSE	-2.21	0.000	0.009
KEGG_CELL_CYCLE	-2.21	0.002	0.009
REACTOME_HIV_LIFE_CYCLE	-2.21	0.002	0.009
REACTOME_MEIOSIS	-2.19	0.002	0.011
REACTOME_G1_S_TRANSITION	-2.19	0.002	0.011
REACTOME_FORMATION_OF_THE_HIV1_EARLY_ELONGATION_COMPLEX	-2.18	0.000	0.011
REACTOME_THE_ROLE_OF_NEF_IN_HIV1_REPLICATION_AND_DISEASE_PATHOGENESIS	-2.18	0.002	0.011
REACTOME_RNA_POL_I_RNA_POL_III_AND_MITOCHONDRIAL_TRANSCRIPTION	-2.17	0.002	0.012
SA_B_CELL_RECEPTOR_COMPLEXES	-2.17	0.004	0.012
BIOCARTA_FCER1_PATHWAY	-2.17	0.000	0.012
PID_ER_NONGENOMIC_PATHWAY	-2.17	0.002	0.012

REACTOME_ACTIVATION_OF_ATR_IN_RESPONSE_TO_REPLICATION_STRESS	-2.16	0.002	0.012
PID_GMCSF_PATHWAY	-2.15	0.002	0.013
PID_TCR_PATHWAY	-2.14	0.000	0.013
REACTOME_TRANSLATION	-2.14	0.002	0.013
REACTOME_TOLL_RECEPTOR_CASCADES	-2.13	0.002	0.014
KEGG_HUNTINGTONS_DISEASE	-2.13	0.004	0.014
KEGG_PYRIMIDINE_METABOLISM	-2.12	0.004	0.015
PID_FCER1_PATHWAY	-2.11	0.002	0.015
PID_RAC1_REG_PATHWAY	-2.11	0.002	0.015
REACTOME_MITOTIC_G1_G1_S_PHASES	-2.11	0.000	0.016
PID_PLK1_PATHWAY	-2.10	0.002	0.016
PID_CASPASE_PATHWAY	-2.10	0.002	0.016
BIOCARTA_RACCYCD_PATHWAY	-2.10	0.002	0.016
REACTOME_PLATELET_AGGREGATION_PLUG_FORMATION	-2.08	0.002	0.018
KEGG_REGULATION_OF_ACTIN_CYTOSKELETON	-2.08	0.002	0.018
BIOCARTA_PDGF_PATHWAY	-2.08	0.006	0.018
PID_S1P_S1P2_PATHWAY	-2.08	0.002	0.018
ST_TUMOR_NECROSIS_FACTOR_PATHWAY	-2.07	0.000	0.018
PID_PI3KCI_PATHWAY	-2.07	0.004	0.018
REACTOME_ENDOSOMAL_SORTING_COMPLEX_REQUIRED_FOR_TRANSPORT_ESCRT	-2.07	0.004	0.018
REACTOME_G_PROTEIN_BETA_GAMMA_SIGNALLING	-2.06	0.008	0.019
REACTOME_ADAPTIVE_IMMUNE_SYSTEM	-2.06	0.004	0.019
REACTOME_RNA_POL_II_TRANSCRIPTION_PRE_INITIATION_AND_PROMOTER_OPENING	-2.06	0.002	0.019
KEGG_OLFACTORY_TRANSDUCTION	-2.05	0.004	0.019
PID_VEGFR1_2_PATHWAY	-2.04	0.000	0.020
SIG_BCR_SIGNALING_PATHWAY	-2.04	0.008	0.020
BIOCARTA_INTEGRIN_PATHWAY	-2.04	0.006	0.021
REACTOME_G1_S_SPECIFIC_TRANSCRIPTION	-2.03	0.004	0.021
BIOCARTA_GLEEVEC_PATHWAY	-2.02	0.002	0.022
PID_ATR_PATHWAY	-2.02	0.002	0.023
PID_ARF6_PATHWAY	-2.01	0.008	0.023
HALLMARK_APOPTOSIS	-2.01	0.008	0.023
HALLMARK_INTERFERON_ALPHA_RESPONSE	-2.01	0.006	0.023
KEGG_SNARE_INTERACTIONS_IN_VESICULAR_TRANSPORT	-2.01	0.006	0.024
BIOCARTA_BCR_PATHWAY	-2.00	0.000	0.024
BIOCARTA_ECM_PATHWAY	-2.00	0.008	0.024
REACTOME_REGULATION_OF_MITOTIC_CELL_CYCLE	-2.00	0.006	0.024
REACTOME_ACTIVATED_TLR4_SIGNALLING	-2.00	0.002	0.025
BIOCARTA_TNFR1_PATHWAY	-1.99	0.006	0.025
ST_T_CELL_SIGNAL_TRANSDUCTION	-1.99	0.006	0.025
REACTOME_IL_2_SIGNALING	-1.99	0.012	0.025
KEGG_EPITHELIAL_CELL_SIGNALING_IN_HELICOBACTER_PYLORI_INFECTION	-1.99	0.008	0.025
KEGG_ALZHEIMERS_DISEASE	-1.98	0.008	0.027
KEGG_CHRONIC_MYELOID_LEUKEMIA	-1.98	0.002	0.027
BIOCARTA_NKCELLS_PATHWAY	-1.98	0.004	0.027
PID_ENDOTHELIN_PATHWAY	-1.97	0.006	0.027

REACTOME_MYD88_MAL_CASCADE_INITIATED_ON_PLASMA_MEMBRANE	-1.97	0.002	0.027
SIG_PIP3_SIGNALING_IN_B_LYMPHOCYTES	-1.97	0.002	0.027
REACTOME_MEIOTIC_RECOMBINATION	-1.97	0.006	0.027
REACTOME_FORMATION_OF_TRANSCRIPTION_COUPLED_NER_TC_NER_REPAIR_COMPLEX	-1.97	0.002	0.027
REACTOME_APC_CDC20_MEDIATED_DEGRADATION_OF_NEK2A	-1.96	0.013	0.027
BIOCARTA_RAS_PATHWAY	-1.96	0.004	0.027
REACTOME_OLFACTORY_SIGNALING_PATHWAY	-1.96	0.004	0.027
REACTOME_CELL_CYCLE_CHECKPOINTS	-1.96	0.004	0.028
REACTOME_PROCESSING_OF_CAPPED_INTRONLESS_PRE_MRNA	-1.95	0.004	0.029
REACTOME_CHOLESTEROL_BIOSYNTHESIS	-1.95	0.006	0.029
HALLMARK_ALLOGRAFT_REJECTION	-1.95	0.010	0.029
KEGG_STEROID_HORMONE_BIOSYNTHESIS	-1.93	0.012	0.032
REACTOME_INTRINSIC_PATHWAY_FOR_APOPTOSIS	-1.93	0.010	0.032
REACTOME_INSULIN_RECEPTOR_RECYCLING	-1.92	0.010	0.034
PID_HIV_NEF_PATHWAY	-1.92	0.012	0.034
REACTOME_TELOMERE_MAINTENANCE	-1.91	0.011	0.034
REACTOME_RECYCLING_PATHWAY_OF_L1	-1.91	0.006	0.034
PID_ALPHA_SYNUCLEIN_PATHWAY	-1.91	0.008	0.035
REACTOME_MITOTIC_G2_G2_M_PHASES	-1.91	0.002	0.035
BIOCARTA_EGF_PATHWAY	-1.91	0.004	0.035
SA_PTEN_PATHWAY	-1.91	0.016	0.035
HALLMARK_PI3K_AKT_MTOR_SIGNALING	-1.90	0.012	0.035
REACTOME_SIGNALING_BY_SCF_KIT	-1.90	0.009	0.036
BIOCARTA_MPR_PATHWAY	-1.90	0.006	0.036
PID_BCR_5PATHWAY	-1.90	0.013	0.037
KEGG_PROGESTERONE_MEDIATED_OOCYTE_MATURATION	-1.89	0.014	0.037
PID_THROMBIN_PAR4_PATHWAY	-1.89	0.014	0.037
REACTOME_SEMAPHORIN_INTERACTIONS	-1.89	0.006	0.037
KEGG_NON_SMALL_CELL_LUNG_CANCER	-1.89	0.004	0.037
REACTOME_METABOLISM_OF_NON_CODING_RNA	-1.89	0.008	0.038
KEGG_RETINOL_METABOLISM	-1.88	0.010	0.038
REACTOME_E2F_MEDIATED_REGULATION_OF_DNA_REPLICATION	-1.88	0.019	0.038
REACTOME_TRANSPORT_OF_MATURE_TRANSCRIPT_TO_CYTOPLASM	-1.88	0.004	0.038
REACTOME_RNA_POL_I_TRANSCRIPTION_INITIATION	-1.88	0.008	0.038
REACTOME_M_G1_TRANSITION	-1.88	0.008	0.037
REACTOME_GASTRIN_CREB_SIGNALLING_PATHWAY_VIA_PKC_AND_MAPK	-1.88	0.008	0.037
PID_P38_MK2_PATHWAY	-1.88	0.014	0.038
PID_NFKAPPAB_ATYPICAL_PATHWAY	-1.88	0.014	0.038
PID_FANCONI_PATHWAY	-1.88	0.012	0.038
PID_LYSOPHOSPHOLIPID_PATHWAY	-1.87	0.024	0.038
BIOCARTA_P38MAPK_PATHWAY	-1.87	0.018	0.039
BIOCARTA_IGF1_PATHWAY	-1.87	0.020	0.040
BIOCARTA_FMLP_PATHWAY	-1.86	0.016	0.040
BIOCARTA_RELA_PATHWAY	-1.86	0.012	0.040
REACTOME_INTERFERON_GAMMA_SIGNALING	-1.86	0.010	0.041
BIOCARTA_EPO_PATHWAY	-1.86	0.022	0.040

REACTOME_ANTIGEN_ACTIVATES_B_CELL_RECEPTOR_LEADING_TO_GENERATION_OF_SECOND_MESSENGERS	-1.86	0.012	0.040
PID_P75_NTR_PATHWAY	-1.85	0.008	0.041
REACTOME_ELONGATION_ARREST_AND_RECOVERY	-1.84	0.020	0.044
ST_ERK1_ERK2_MAPK_PATHWAY	-1.83	0.017	0.045
REACTOME_NFKB_AND_MAP_KINASES_ACTIVATION_MEDIATED_BY_TLR4_SIGNALING_REPERTOIRE	-1.83	0.020	0.045
PID_CMYB_PATHWAY	-1.83	0.018	0.046
REACTOME_FACTORS_INVOLVED_IN_MEGAKARYOCYTE_DEVELOPMENT_AND_PLATELET_PRODUCTION	-1.83	0.012	0.046
PID_AR_NONGENOMIC_PATHWAY	-1.83	0.016	0.046
REACTOME_IL_3_5_AND_GM_CSF_SIGNALING	-1.83	0.016	0.046
KEGG_AMINO_SUGAR_AND_NUCLEOTIDE_SUGAR_METABOLISM	-1.82	0.014	0.046
SIG_CHEMOTAXIS	-1.82	0.014	0.046
KEGG_MISMATCH_REPAIR	-1.82	0.012	0.046
KEGG_ASTHMA	-1.82	0.022	0.047
PID_IL6_7_PATHWAY	-1.82	0.008	0.047
BIOCARTA_IL2RB_PATHWAY	-1.82	0.008	0.047
PID_TOLL_ENDOGENOUS_PATHWAY	-1.82	0.021	0.047
KEGG_RENAL_CELL_CARCINOMA	-1.82	0.014	0.047
ST_FAS_SIGNALING_PATHWAY	-1.81	0.020	0.048
REACTOME_MRNA_3_END_PROCESSING	-1.81	0.014	0.048
REACTOME_G0_AND_EARLY_G1	-1.81	0.013	0.048
BIOCARTA_UCALPAIN_PATHWAY	-1.81	0.015	0.048
SIG_REGULATION_OF_THE_ACTIN_CYTOSKELETON_BY_RHO_GTPASES	-1.80	0.020	0.049
PID_CERAMIDE_PATHWAY	-1.80	0.024	0.049
KEGG_HOMOLOGOUS_RECOMBINATION	-1.79	0.026	0.051
BIOCARTA_PYK2_PATHWAY	-1.79	0.016	0.051
BIOCARTA_IL6_PATHWAY	-1.79	0.024	0.052
PID_HDAC_CLASSII_PATHWAY	-1.79	0.018	0.051
REACTOME_APC_C_CDC20_MEDIATED_DEGRADATION_OF_MITOTIC_PROTEINS	-1.79	0.020	0.052
REACTOME_RAP1_SIGNALLING	-1.79	0.026	0.052
REACTOME_CELL_DEATH_SIGNALLING_VIA_NRAGE_NRIF_AND_NADE	-1.78	0.021	0.053
KEGG_TOLL_LIKE_RECEPTOR_SIGNALING_PATHWAY	-1.78	0.022	0.053
KEGG_PENTOSE_AND_GLUCURONATE_INTERCONVERSIONS	-1.78	0.017	0.053
REACTOME_ANTIVIRAL_MECHANISM_BY_IFN_STIMULATED_GENES	-1.78	0.022	0.053
KEGG_VEGF_SIGNALING_PATHWAY	-1.78	0.014	0.053
REACTOME_SHC1_EVENTS_IN_EGFR_SIGNALING	-1.77	0.014	0.055
PID_MET_PATHWAY	-1.77	0.014	0.055
BIOCARTA_FAS_PATHWAY	-1.77	0.016	0.056
KEGG_COLORECTAL_CANCER	-1.76	0.016	0.056
BIOCARTA_TFF_PATHWAY	-1.76	0.018	0.056
REACTOME_SIGNAL_TRANSDUCTION_BY_L1	-1.76	0.018	0.057
KEGG_PENTOSE_PHOSPHATE_PATHWAY	-1.76	0.020	0.057
KEGG_GALACTOSE_METABOLISM	-1.75	0.026	0.058
BIOCARTA_ACTINY_PATHWAY	-1.75	0.016	0.059
HALLMARK_MTORC1_SIGNALING	-1.75	0.021	0.059
BIOCARTA_CXCR4_PATHWAY	-1.75	0.026	0.060

REACTOME_ERK_MAPK_TARGETS	-1.75	0.025	0.060
REACTOME_GLOBAL_GENOMIC_NER_GG_NER	-1.74	0.012	0.061
REACTOME_INHIBITION_OF_THE_PROTEOLYTIC_ACTIVITY_OF_APC_C_REQUIRED_FOR_THE_ONSET_OF_ANAPHASE_BY_MITOTIC_SPINDLE_CHECKPOINT_COMPONENTS	-1.73	0.024	0.063
REACTOME_APC_C_CDH1_MEDIATED_DEGRADATION_OF_CDC20_AND_OTHER_APC_C_CDH1_TARGETED_PROTEINS_IN_LATE_MITOSIS_EARLY_G1	-1.73	0.026	0.063
REACTOME_METABOLISM_OF_NUCLEOTIDES	-1.73	0.022	0.063
BIOCARTA_CCR3_PATHWAY	-1.73	0.030	0.064
HALLMARK_MYC_TARGETS_V2	-1.73	0.016	0.064
KEGG_BASE_EXCISION_REPAIR	-1.72	0.027	0.065
PID_CXCR3_PATHWAY	-1.72	0.038	0.065
REACTOME_TRIF_MEDIATED_TLR3_SIGNALING	-1.72	0.027	0.066
BIOCARTA_MAL_PATHWAY	-1.72	0.024	0.067
REACTOME_PI_METABOLISM	-1.71	0.032	0.067
REACTOME_ABORTIVE_ELONGATION_OF_HIV1_TRANSCRIPT_IN_THE_ABSENCE_OF_TAT	-1.71	0.028	0.067
REACTOME_REGULATION_OF_SIGNALING_BY_CBL	-1.71	0.025	0.067
PID_HEDGEHOG_GLI_PATHWAY	-1.71	0.030	0.067
REACTOME_SHC_RELATED_EVENTS	-1.71	0.028	0.068
KEGG_PURINE_METABOLISM	-1.70	0.029	0.070
REACTOME_MRNA_CAPPING	-1.70	0.031	0.071
REACTOME_DEPOSITION_OF_NEW_CENPA_CONTAINING_NUCLEOSOMES_AT_THE_CENTROMERE	-1.70	0.027	0.071
PID_ARF6_DOWNSTREAM_PATHWAY	-1.70	0.037	0.071
PID_RHOA_PATHWAY	-1.70	0.032	0.071
REACTOME_RNA_POL_I_TRANSCRIPTION_TERMINATION	-1.70	0.018	0.071
REACTOME_SIGNALLING_TO_ERKS	-1.70	0.026	0.071
REACTOME_APC_C_CDC20_MEDIATED_DEGRADATION_OF_CYCLIN_B	-1.69	0.026	0.071
REACTOME_AUTODEGRADATION_OF_CDH1_BY_CDH1_APC_C	-1.69	0.026	0.071
SIG_INSULIN_RECEPTOR_PATHWAY_IN_CARDIAC_MYOCYTES	-1.69	0.028	0.071
ST_PHOSPHOINOSITIDE_3_KINASE_PATHWAY	-1.69	0.030	0.073
REACTOME_BASE_EXCISION_REPAIR	-1.69	0.035	0.073
REACTOME_APOPTOSIS	-1.68	0.019	0.074
SA_MMP_CYTOKINE_CONNECTION	-1.68	0.021	0.074
PID_IL3_PATHWAY	-1.68	0.033	0.075
REACTOME_G_ALPHA1213_SIGNALLING_EVENTS	-1.68	0.020	0.075
REACTOME_SIGNALING_BY_RHO_GTPASES	-1.67	0.037	0.077
BIOCARTA_IGF1R_PATHWAY	-1.66	0.033	0.081
KEGG_PEROXISOME	-1.66	0.034	0.081
BIOCARTA_GH_PATHWAY	-1.66	0.042	0.081
KEGG_MAPK_SIGNALING_PATHWAY	-1.66	0.030	0.082
REACTOME_ACTIVATION_OF_BH3_ONLY_PROTEINS	-1.66	0.029	0.081
REACTOME_TRANS_GOLGI_NETWORK_VESICLE_BUDDING	-1.66	0.036	0.082
REACTOME_RESOLUTION_OF_AP_SITES_VIA_THE_MULTIPLE_NUCLEOTIDE_PATCH_REPLACEMENT_PATHWAY	-1.65	0.030	0.082
BIOCARTA_CHEMICAL_PATHWAY	-1.65	0.034	0.083
BIOCARTA_INSULIN_PATHWAY	-1.65	0.037	0.084
REACTOME_SIGNALING_BY_NOTCH	-1.64	0.027	0.087
REACTOME_INTEGRIN_ALPHAIIB_BETA3_SIGNALING	-1.64	0.038	0.088

KEGG_PARKINSONS_DISEASE	-1.63	0.042	0.090
BIOCARTA_HSP27_PATHWAY	-1.63	0.045	0.092
REACTOME_PHOSPHORYLATION_OF_THE_APC_C	-1.62	0.037	0.092
REACTOME_GOLGI_ASSOCIATED_VESICLE_BIOGENESIS	-1.62	0.039	0.094
REACTOME_SIGNAL_AMPLIFICATION	-1.62	0.024	0.094
REACTOME_NUCLEAR_EVENTS_KINASE_AND_TRANSCRIPTION_FACTOR_ACTIVATION	-1.62	0.041	0.094
PID_E2F_PATHWAY	-1.62	0.031	0.094
KEGG_OOCYTE_MEIOSIS	-1.61	0.044	0.096
PID_EPO_PATHWAY	-1.61	0.040	0.096
REACTOME_HOST_INTERACTIONS_OF_HIV_FACTORS	-1.61	0.033	0.096
BIOCARTA_IL2_PATHWAY	-1.61	0.033	0.098
REACTOME_NEGATIVE_REGULATION_OF_FGFR_SIGNALING	-1.60	0.045	0.099
REACTOME_ACTIVATED_AMPK_STIMULATES_FATTY_ACID_OXIDATION_IN_MUSCLE	-1.60	0.040	0.102
REACTOME_G_BETA_GAMMA_SIGNALLING_THROUGH_PI3KGAMMA	-1.59	0.037	0.105
HALLMARK_REACTIVE_OXIGEN_SPECIES_PATHWAY	-1.59	0.047	0.105
KEGG_GLIOMA	-1.59	0.047	0.106
KEGG_NUCLEOTIDE_EXCISION_REPAIR	-1.58	0.046	0.110
REACTOME_CONVERSION_FROM_APC_C_CDC20_TO_APC_C_CDH1_IN_LATE_ANAPHASE	-1.56	0.044	0.117
REACTOME_ER_PHAGOSOME_PATHWAY	-1.55	0.049	0.119
REACTOME_SHC1_EVENTS_IN_ERBB4_SIGNALING	-1.55	0.050	0.119
KEGG_TYPE_I_DIABETES_MELLITUS	-1.55	0.045	0.119
HALLMARK_GLYCOLYSIS	-1.54	0.045	0.127

Supplemental Table 4. Expression of 80 chemokines, cytokines, growth factors and adhesion molecules in the supernatant fraction and cell fraction of bone marrow from *Sbds*$^{l/l}$ and *Mx1*^{Cre}*Sbds*^{Exc} mice at 48 hours after TBI and baseline measured by ELISA

	Supernatant fraction: 48 hours after TBI			**Cell fraction: 48 hours after TBI**		
	***Sbds*$^{l/l}$**	***Mx1*^{Cre}*Sbds*^{Exc}**		***Sbds*$^{l/l}$**	***Mx1*^{Cre}*Sbds*^{Exc}**	
Protein	**Mean ± SD (pg/mL)**	**Mean ± SD (pg/mL)**	**P value**	**Mean ± SD (pg/mL)**	**Mean ± SD (pg/mL)**	**P value**
AR	6.8 ± 9.9	15.9 ± 15.5	0.318	0 ± 0	3.2 ± 6.4	0.356
Axl	154.6 ± 64.0	118.5 ± 155.2	0.651	10.6 ± 15.5	0 ± 0	0.221
CD27L	65.5 ± 61.1	2.1 ± 2.6	0.065	0 ± 0	0 ± 0	N/A
CD30 (TNFRSF8)	72.1 ± 45.0	98.6 ± 35.3	0.358	0 ± 0	2.2 ± 4.5	0.356
CD40 (TNFRSF5)	6.0 ± 9.7	8.1 ± 16.3	0.809	0 ± 0	2.1 ± 4.2	0.356
CXCL16	48.6 ± 8.7	51.6 ± 7.0	0.592	1 ± 1.2	1.2 ± 2.4	0.886
EGF	5.0 ± 7.3	0.0 ± 0.0	0.199	1.2 ± 1.7	0.3 ± 0.7	0.342
E-selectin	190.4 ± 54.0	749.5 ± 328.5	0.005*	0 ± 0	1.9 ± 2.2	0.136
Fractalkine (CX3CL1)	243.7 ± 173.8	170.5 ± 125.6	0.495	0 ± 0	0 ± 0	N/A
GITR (TNFRSF18)	814.9 ± 88.0	720.3 ± 113.1	0.192	16.6 ± 15.8	16.2 ± 16.1	0.975
HGF	1090.1 ± 256.3	1845.6 ± 720.7	0.059	134.6 ± 279.8	257 ± 358.7	0.542
IGFBP-2	1060.6 ± 233.0	2080.4 ± 704.0	0.015*	11.3 ± 13.3	30.8 ± 27	0.137
IGFBP-3	8478.7 ± 1666.8	12996.3 ± 3051.6	0.020*	354.2 ± 457.2	729 ± 546.4	0.252
IGFBP-5	694.3 ± 192.1	413.1 ± 98.2	0.025*	35.8 ± 20.6	42.1 ± 20.9	0.680
IGFBP-6	1884.5 ± 739.5	1498.3 ± 243.2	0.338	3.6 ± 4.4	9.4 ± 18.3	0.556
IGF-I	79821.2 ± 13483.7	36653.5 ± 15988.1	0.002*	313.4 ± 460	449.9 ± 563.1	0.671
IL-12p70	599.8 ± 309.5	497.1 ± 197.8	0.576	6.9 ± 12.3	17.9 ± 21.2	0.295
IL-17E (IL-25)	55.1 ± 52.8	73.0 ± 48.2	0.612	8.8 ± 18.6	14.7 ± 24.2	0.658
IL-17F	45.3 ± 51.5	61.3 ± 22.7	0.574	10.4 ± 27.4	18.1 ± 36.2	0.695
IL-1ra (IL-1 F3)	20.8 ± 5.5	100.8 ± 44.8	0.004*	0.6 ± 1.1	0.8 ± 1.5	0.809
IL-2 Ra	23.8 ± 31.8	11.8 ± 6.8	0.473	0 ± 0	0 ± 0	N/A
IL-20	565.4 ± 128.6	490.6 ± 71.7	0.322	109.7 ± 105.4	166.3 ± 120	0.435
IL-23	1407.0 ± 727.2	1116.5 ± 178.9	0.451	68.2 ± 136.3	0 ± 0	0.356
IL-28	62.1 ± 43.8	51.3 ± 19.6	0.655	3.7 ± 4.7	6.6 ± 4	0.369
I-TAC (CXCL11)	185.7 ± 79.3	184.6 ± 102.4	0.986	0 ± 0	0 ± 0	N/A
MDC (CCL22)	4.8 ± 2.0	1.4 ± 0.9	0.012*	0.3 ± 0.5	0 ± 0	0.300
MIP-2	37.8 ± 29.2	31.4 ± 17.6	0.703	8.4 ± 4.9	15.4 ± 8.3	0.107
MIP-3a (CCL20)	17.0 ± 9.7	24.3 ± 11.2	0.323	0 ± 0	0 ± 0	N/A
OPN (SPP1)	7389.3 ± 503.3	10602.6 ± 973.6	0.000*	2945.3 ± 1783.8	3126.7 ± 1086.6	0.868
OPG	335.6 ± 111.7	216.5 ± 40.1	0.071	20.5 ± 12.8	14.4 ± 9.4	0.426
Prolactin	41.8 ± 28.8	104.9 ± 53.5	0.051	0 ± 0	2.9 ± 5.8	0.356
Pro-MMP-9	50011.4 ± 13711.6	38635.5 ± 11850.6	0.220	43475.3 ± 26090.7	58209.4 ± 19248.1	0.398
P-selectin	37660.7 ± 14127.8	24742.6 ± 10982.2	0.166	6927.8 ± 1587.2	2679.1 ± 1816.9	0.012*
Resistin	339.0 ± 82.0	431.5 ± 72.8	0.110	13.5 ± 8	25.4 ± 5.9	0.053
SCF	10.7 ± 10.3	5.1 ± 4.6	0.338	2 ± 3	1.7 ± 2.3	0.852
SDF-1a (CXCL12)	606.0 ± 148.2	184.6 ± 58.6	0.000*	16.2 ± 11.4	11.2 ± 10.3	0.489
TPO	296.4 ± 200.3	394.8 ± 247.3	0.526	0.7 ± 1.8	1.2 ± 2.3	0.695
VCAM-1 (CD106)	2831.1 ± 682.6	4683.0 ± 1362.7	0.027*	1979.8 ± 1334.4	2198.4 ± 1780.4	0.821
VEGF	138.4 ± 105.0	56.9 ± 30.2	0.163	61.5 ± 82.6	84.1 ± 101.4	0.696

VEGF-D	17.4 ± 7.3	10.4 ± 1.8	0.094	0 ± 0	0.6 ± 1.2	0.356
bFGF	133.3 ± 34.8	98.0 ± 26.3	0.125	157 ± 49	205.7 ± 77.7	0.330
BLC (CXCL13)	39.1 ± 25.1	211.8 ± 124.0	0.015*	81.3 ± 44.9	197.8 ± 96.5	0.071
CD30L	381.7 ± 498.9	59.8 ± 60.5	0.227	19.2 ± 38.4	35.2 ± 70.4	0.704
Eotaxin(CCL11)	95.1 ± 41.1	42.0 ± 24.8	0.048*	241.2 ± 60	165.6 ± 74.3	0.164
Eotaxin-2 (CCL24)	65.3 ± 24.2	52.3 ± 20.2	0.408	59.6 ± 41.3	54.3 ± 13.4	0.815
Fas L (TNFSF6)	7.8 ± 10.1	1.7 ± 1.4	0.257	16.5 ± 14.3	18.3 ± 15	0.867
G-CSF	3.0 ± 6.5	5.0 ± 10.0	0.721	37.5 ± 54.8	126.9 ± 108.9	0.192
GM-CSF	267.3 ± 407.7	821.3 ± 537.8	0.113	423.1 ± 846.2	618.9 ± 1028.7	0.779
ICAM-1 (CD54)	1768.2 ± 923.1	2115.9 ± 768.4	0.559	28987.1 ± 770.5	35345.2 ± 17872.8	0.538
IFNg	3984.9 ± 3248.3	2072.7 ± 844.6	0.277	2727.8 ± 3109.3	1643.4 ± 1244.8	0.541
IL-1a	60.3 ± 42.2	56.5 ± 18.1	0.867	51.7 ± 52.5	54.7 ± 37.6	0.929
IL-1b	0.7 ± 0.7	0.4 ± 0.4	0.440	10.9 ± 12.5	5.3 ± 7.7	0.476
IL-2	934.7 ± 883.7	340.4 ± 132.1	0.211	135.2 ± 133.8	58.7 ± 67.1	0.346
IL-3	18.9 ± 27.6	35.5 ± 27.7	0.393	22.3 ± 44.5	14.6 ± 29.3	0.784
IL-4	0.9 ± 1.6	0.2 ± 0.5	0.411	5.8 ± 7.0	9.1 ± 14.8	0.704
IL-5	17.5 ± 39.0	5.0 ± 10.0	0.544	17.6 ± 35.1	6.7 ± 13.4	0.584
IL-6	296.4 ± 399.4	15.7 ± 20.2	0.189	90.1 ± 180.2	3.5 ± 7	0.374
IL-7	2.4 ± 2.5	4.1 ± 4.1	0.463	10.4 ± 13.1	3.3 ± 2.3	0.328
IL-10	20.8 ± 30.5	13.0 ± 16.0	0.649	70.2 ± 76.7	111.4 ± 109.1	0.559
IL-12p40	49.1 ± 81.0	8.2 ± 8.3	0.336	9.5 ± 9.5	6.3 ± 7.9	0.629
IL-13	7243.5 ± 5738.2	10485.1 ± 6015.6	0.430	11385.7 ± 7702.1	10079 ± 3941.4	0.773
IL-15	1600.2 ± 2040.9	3386.4 ± 1786.1	0.200	2880.4 ± 3640.8	2951 ± 5168	0.983
IL-17	6.1 ± 7.6	8.1 ± 9.7	0.737	5 ± 10	4.6 ± 9.3	0.962
IL-21	5.3 ± 6.9	5.0 ± 3.5	0.935	26.7 ± 18.1	13.9 ± 20.5	0.386
KC (CXCL1)	127.5 ± 106.3	10.6 ± 10.6	0.054	205.1 ± 238.7	222.9 ± 247.3	0.921
Leptin	616.3 ± 288.9	383.3 ± 279.2	0.252	0.9 ± 1.2	0.1 ± 0.2	0.250
LIX(CXCL5)	21.4 ± 33.0	0.0 ± 0.0	0.222	3925.5 ± 5449.2	3160.7 ± 5465.1	0.849
MCP-1 (CCL2)	47.7 ± 46.0	28.5 ± 35.5	0.508	161.8 ± 186.6	173.2 ± 136.4	0.925
MCP-5 (CCL12)	117.8 ± 57.8	81.0 ± 32.6	0.282	180.5 ± 96.1	157.5 ± 98.4	0.749
M-CSF	54.6 ± 37.8	17.3 ± 19.4	0.104	170.7 ± 195.8	114.9 ± 128	0.650
MIG (CXCL9)	9407.8 ± 3597.8	1924.8 ± 1027.7	0.003*	7122.9 ± 3814.1	3559.4 ± 1128.6	0.123
MIP-1a (CCL3)	79.2 ± 41.1	304.4 ± 188.9	0.030*	282.1 ± 110.4	307.9 ± 140.9	0.783
MIP-1g (CCL9)	726.2 ± 224.6	2432.4 ± 1057.5	0.007*	1667.7 ± 806.1	4753.1 ± 630.6	0.001*
PF-4	453484.1 ± 172603.4	328754.0 ± 126816.7	0.256	313168.2 ± 110551.5	396393.1 ± 47056.1	0.385
RANTES (CCL5)	210.6 ± 86.5	160.6 ± 94.2	0.429	947.2 ± 274.6	485.7 ± 107.1	0.020*
TARC (CCL17)	100.4 ± 126.3	180.6 ± 86.4	0.305	196.3 ± 167.2	213.1 ± 150.9	0.886
TCA-3 (CCL1)	0.0 ± 0.0	0.0 ± 0.0	NA	0 ± 0	77.6 ± 98.4	0.166
TNF RI (TNFRSF1A)	295.5 ± 64.4	246.0 ± 89.6	0.362	716.3 ± 552	837.8 ± 701.6	0.795
TNF RII (TNFRSF1B)	186.7 ± 69.8	152.1 ± 58.4	0.446	112.4 ± 159.1	97.3 ± 147.2	0.893
TNFa	3.3 ± 4.7	0.9 ± 1.7	0.349	0 ± 0	0 ± 0	N/A
	Supernatant fraction: baseline			**Cell fraction: baseline**		
CD27L	5.7 ± 3.5	8.4 ± 4.6	0.267	8.8 ± 10.9	10 ± 5.3	0.827
E-selectin	28.7 ± 20.4	20 ± 2	0.373	7.2 ± 3	8.2 ± 2.4	0.553
HGF	315.7 ± 206.0	216.8 ± 117.3	0.360	760.6 ± 315.1	451.5 ± 302.2	0.119
IGFBP-2	28 ± 17.4	56.6 ± 46.5	0.162	41.5 ± 20.2	43.3 ± 53.8	0.936

IGFBP-3	365.3 ± 174.1	273.5 ± 27.9	0.276	20.3 ± 8.3	16 ± 8.2	0.395
IGFBP-5	416 ± 127.2	816.3 ± 110.2	0.0002*	153.7 ± 141.3	86 ± 40.9	0.328
IGF-I	96 ± 40.4	215.5 ± 73.5	0.005*	0.4 ± 0.2	3.2 ± 4.8	0.144
IL-1ra (IL-1 F3)	3.2 ± 1	3 ± 1	0.802	2 ± 1.5	1.6 ± 1.6	0.637
MDC (CCL22)	4.3 ± 2	6.9 ± 2.6	0.075	1.7 ± 0.5	1.8 ± 0.6	0.866
MIP-3a (CCL20)	1.3 ± 0.9	0.8 ± 0.6	0.259	0.5 ± 0.4	0.7 ± 0.3	0.395
OPN (SPP1)	2708.2 ± 1135.3	3242 ± 1644.8	0.519	41.8 ± 23.4	63.1 ± 32.2	0.212
OPG	180.1 ± 112.6	148 ± 41.5	0.561	30.2 ± 16.9	28.5 ± 7.4	0.840
P-selectin	1449.4 ± 376.7	2145.2 ± 813.1	0.072	1793.7 ± 827	1442.1 ± 1120	0.544
SDF-1a (CXCL12)	32.6 ± 16.8	35.4 ± 23.7	0.812	7.3 ± 2.8	13.3 ± 7.4	0.076
VCAM-1 (CD106)	2701 ± 564.7	2926 ± 712.1	0.554	2722.1 ± 926.7	2293.3 ± 1468.2	0.550
VEGF	5.1 ± 2.8	7 ± 3.7	0.336	20.4 ± 6.6	14.8 ± 2.9	0.107
BLC (CXCL13)	10.4 ± 4.8	7.7 ± 4.4	0.346	7.1 ± 4.4	8.5 ± 1.9	0.532
G-CSF	0.0 ± 0.1	0.1 ± 0.2	0.299	0.4 ± 0.5	1.1 ± 0.6	0.071
GM-CSF	8.4 ± 5.5	4.9 ± 3.5	0.246	39.7 ± 7.7	36.7 ± 13.1	0.631
IL-5	6.9 ± 8.9	15.5 ± 14.2	0.223	13.5 ± 21.9	40 ± 12.6	0.036*
KC (CXCL1)	4.1 ± 4.6	5.3 ± 5.2	0.677	12.3 ± 5	24.7 ± 9.5	0.015*
Leptin	14 ± 16.1	78.6 ± 24	0.000*	4.5 ± 5.2	16 ± 9.6	0.022*
M-CSF	0.2 ± 0.1	0.3 ± 0.5	0.482	1.7 ± 3.5	0.5 ± 0.5	0.455
MIG (CXCL9)	88.5 ± 37.1	109 ± 22.6	0.301	43.8 ± 22.3	73.2 ± 22.4	0.048*
MIP-1a (CCL3)	13.1 ± 7.2	14.5 ± 7.1	0.760	25.8 ± 7.3	27.7 ± 8.4	0.687
MIP-1g (CCL9)	115.2 ± 46.3	100 ± 42.6	0.575	508.4 ± 116.7	345.2 ± 217.1	0.121
RANTES (CCL5)	47.4 ± 30.4	78.2 ± 27.4	0.101	5.6 ± 4.3	7 ± 3.6	0.572

* $p<0.05$, Student's t-test.

Supplemental Figure 1

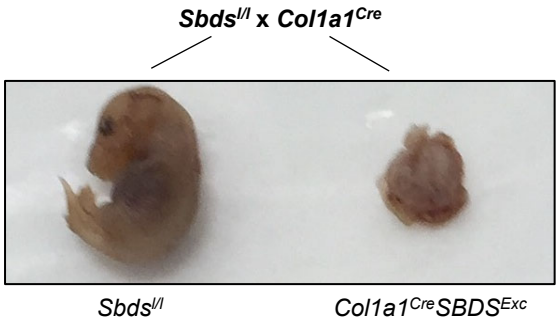

Supplemental Figure 2

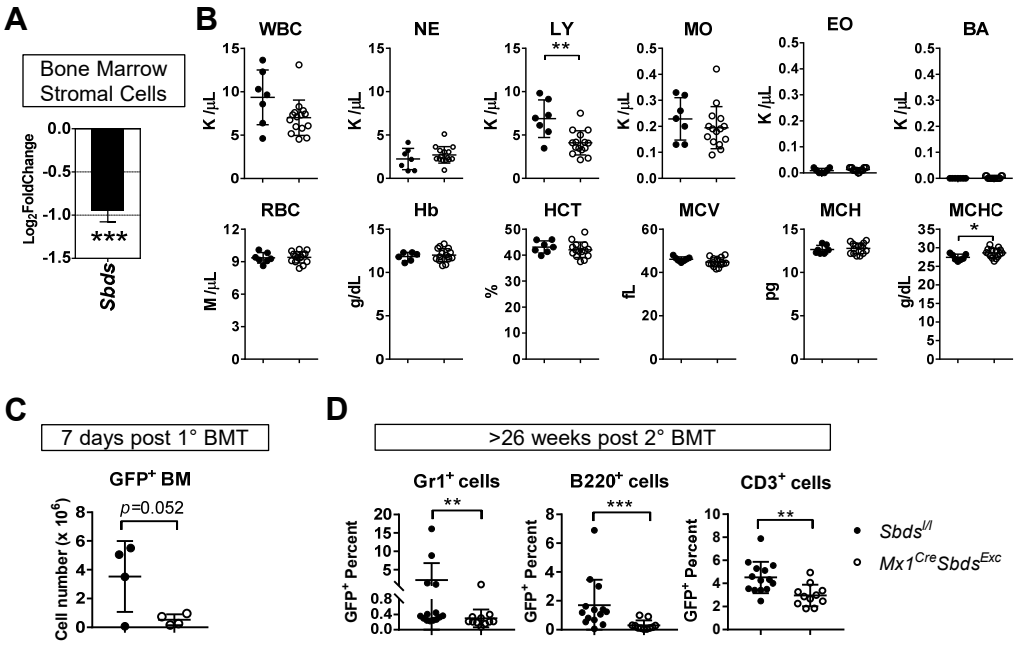

Supplemental Figure 3

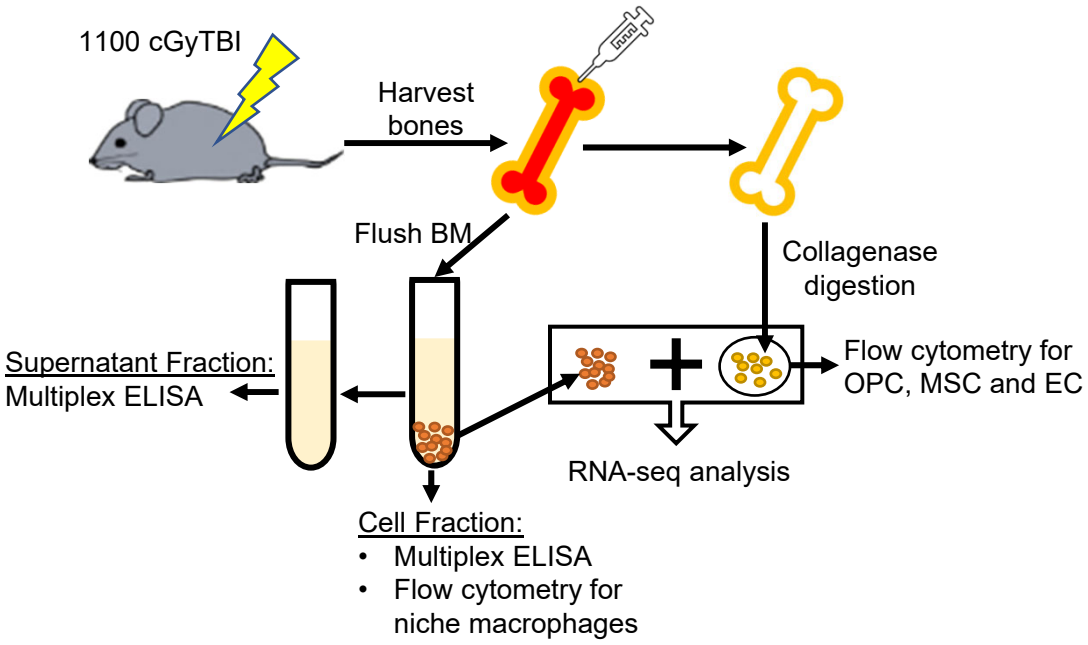

Supplemental Figure 4

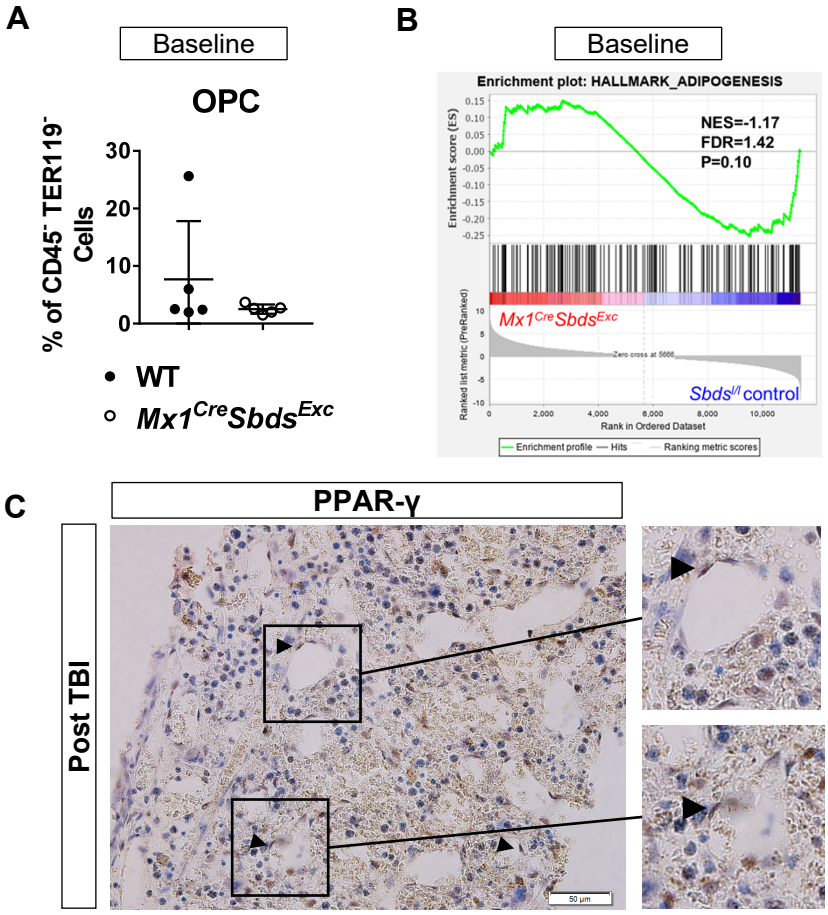

Supplemental Figure 5

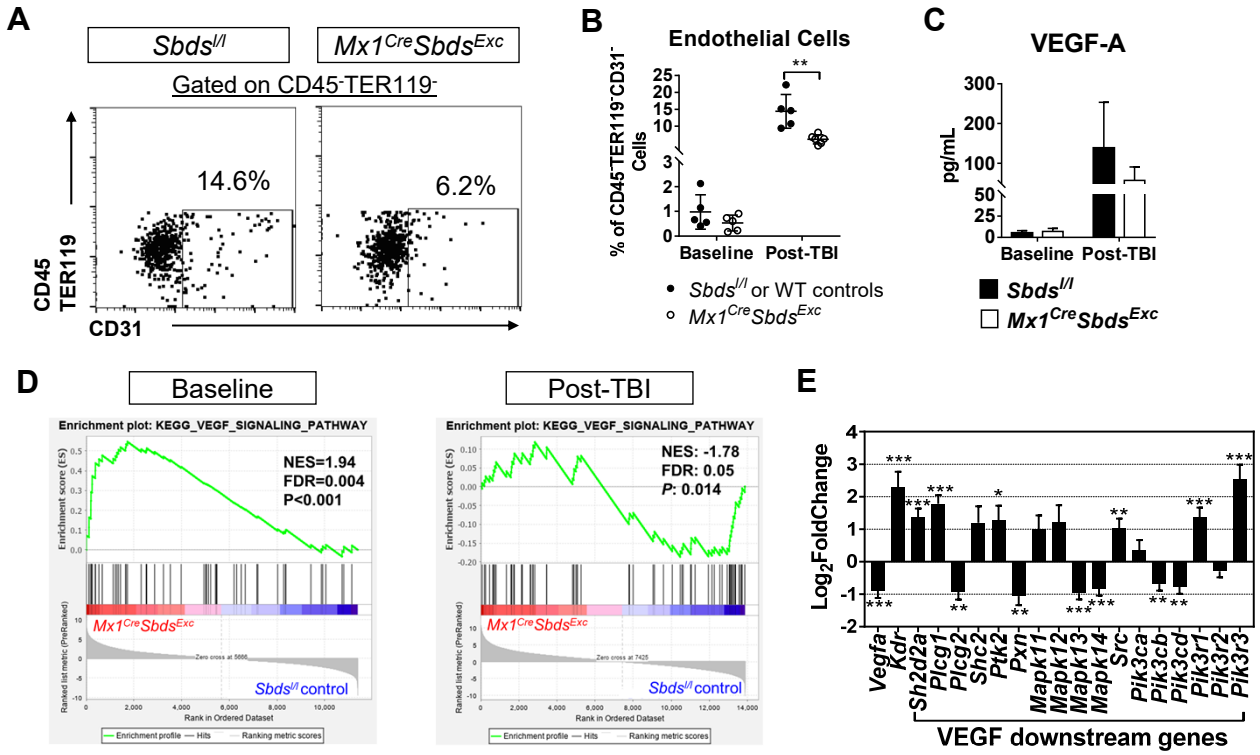

Supplemental Figure 6

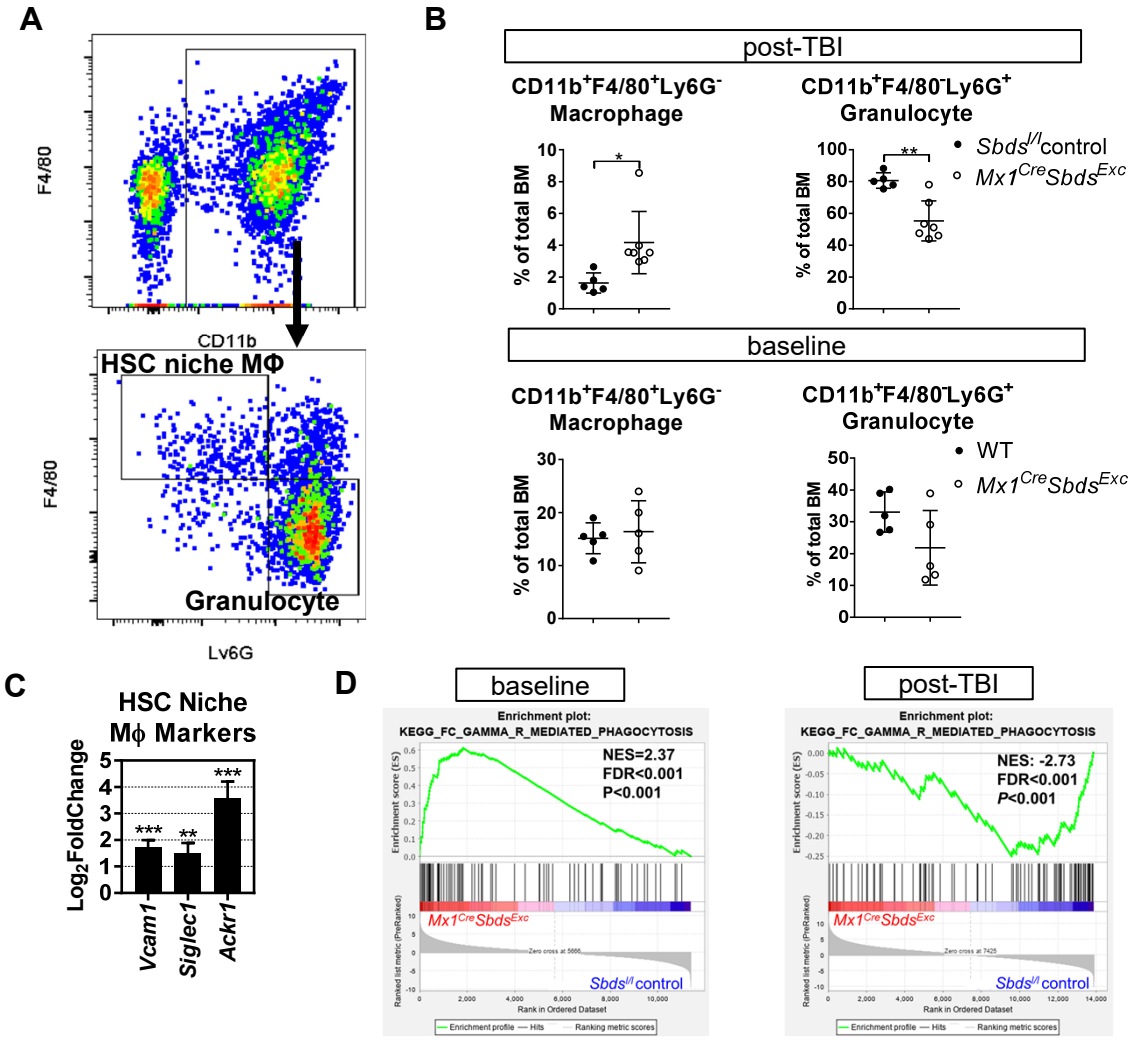

Supplemental Figure 7

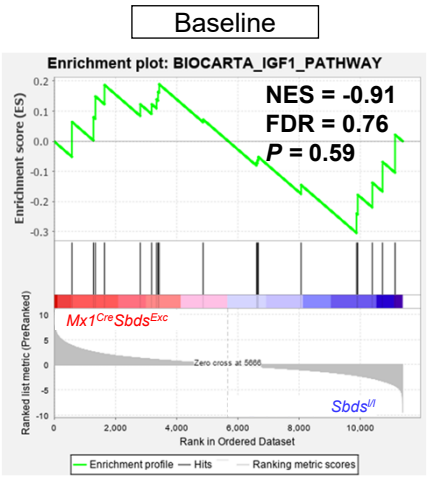

Supplemental Figure 8

A baseline

	NES	FDR	*P* Value
KEGG_RIBOSOME	0.85	0.83	0.711
REACTOME_PEPTIDE_CHAIN_ELONGATION	0.86	0.81	0.713

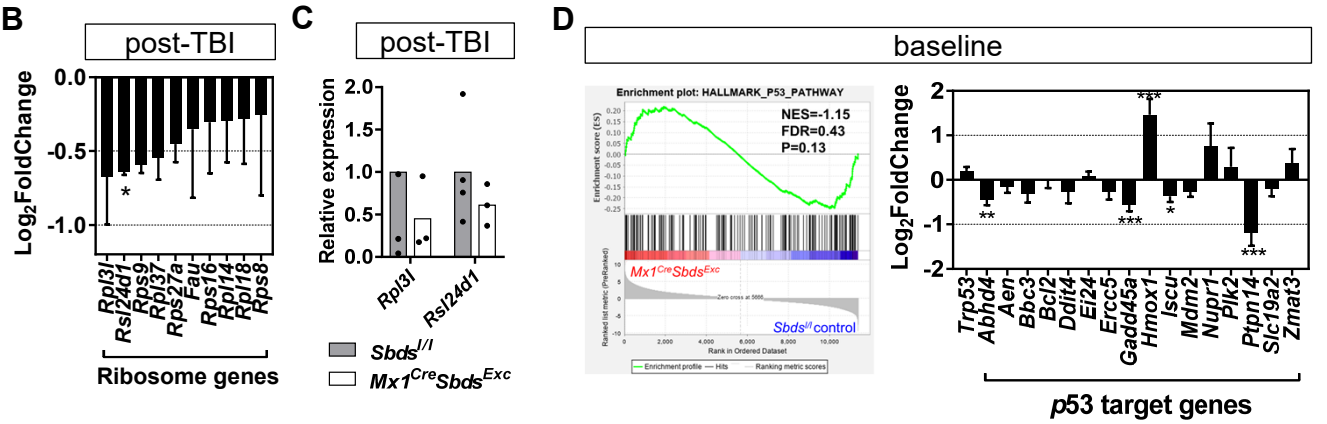

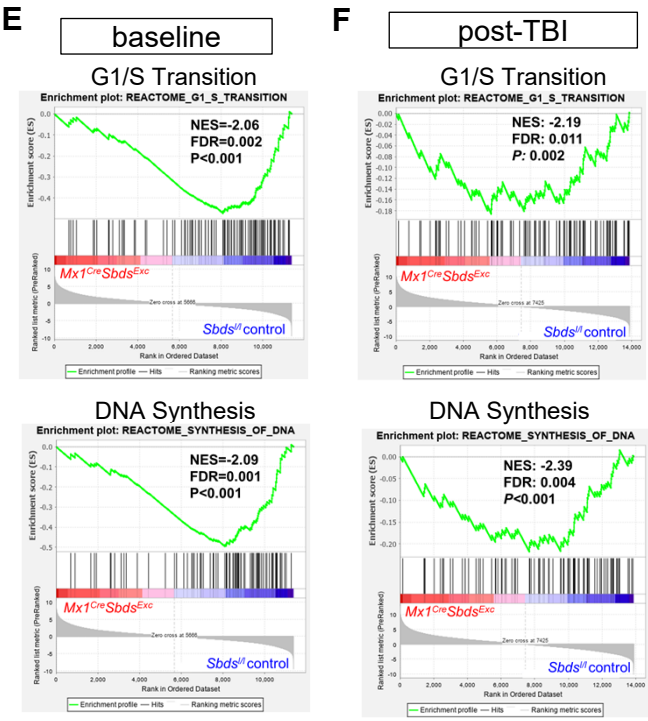

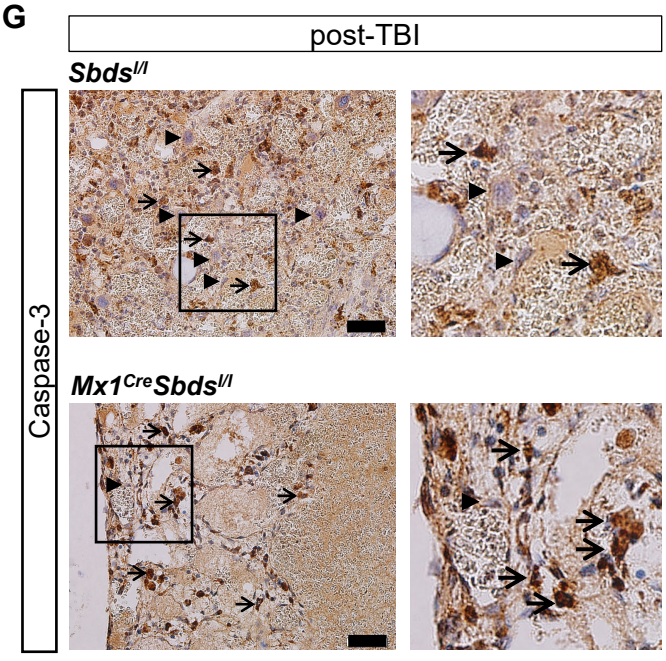

Supplemental Figure 1: Developmental Defects in *col1a1^{Cre}Sbds^{Exc}* strain. Representative images of *Sbds$^{l/l}$* and *col1a1^{Cre}Sbds^{Exc}* fetuses at embryonic stage E12-E15, showing severe developmental skeletal abnormalities prohibiting viability. No pups with the *col1a1^{Cre}Sbds^{Exc}* genotype survived to delivery.

Supplemental Figure 2: *Mx1^{Cre}Sbds^{Exc}* mice exhibit disrupted hematopoiesis and impaired niche capacity to engraft donor HSC. (A) Expression of Sbds mRNA in isolated CD45^{neg} BM stromal cells is reduced in *Mx1^{Cre}Sbds^{Exc}* mice compared to Sbds$^{l/l}$ controls, as shown in RNA-seq analysis. ***p<0.001, *DESeq2* statistical test. **(B)** Complete blood count analysis of white blood cells (WBC), neutrophils (NE), lymphocytes (LY), monocytes (MO), eosinophils (EO), basophils (BA), red blood cells (RBC), hemoglobin (Hb), hematocrit (HCT), mean corpuscular volume (MCV), mean corpuscular hemoglobin (MCH) and mean corpuscular hemoglobin concentration (MCHC) in Sbds$^{l/l}$ (n=7) and Mx1^{Cre}Sbds^{Exc} mice (n=12). 100 microliter peripheral blood was collected from retro-orbital plexus of the mice anesthetized under isoflurane and stored in microcentrifuge tubes containing EDTA. Complete blood counts were analyzed using Hemavet 950FS (Drew Scientific Group). *p<0.05, **p<0.01, Student's t-test. **(C)** Mx1^{Cre}Sbds^{Exc} primary recipients exhibit low numbers of engrafted healthy GFP^{+} donor BM cells compared to Sbds$^{l/l}$ control recipients at 1 week post-BMT (n=4 mice per group). **(D)** Examination of GFP^{+} cell percentages within BM cell populations in WT secondary recipients beyond 26 weeks post-secondary BMT. These secondary recipients had received WT competitor BM plus either Mx1^{Cre}Sbds^{Exc} or control (Sbds$^{l/l}$) primary recipient BM marrow collected 7 days after these primary recipients had undergone myeloablative BMT using GFP^{+} donor BM. (n=4 primary recipients and n =14 secondary recipients per group). HSC engraftment in primary recipient Mx1^{Cre}Sbds^{Exc} mice was significantly impaired, as indicated by lower GFP^{+} reconstitution of secondary recipient trilineage BM hematopoiesis, including Gr1^{+} myeloid cells, B220^{+} B cells, and CD3^{+} T cells. **p<0.01, ***p<0.001, Mann-Whitney test.

Supplemental Figure 3: Experimental Scheme defining sample collections for ELISA and RNA-seq analysis on the BM niche of irradiated mice. For ELISA analysis, BM was flushed out from femora and tibiae of mice 48 hours after 1100cGy TBI using a constant volume of PBS per bone to enable intragroup and interstrain comparisons of extracellular protein levels. The cell suspension was centrifuged, and the BM plasma supernatant and BM cell fractions were applied without dilution for multiplex ELISA analysis separately. For RNA-seq analysis and flow cytometry analysis of BM niche cells, after non-adherent BM was flushed out at 24 hours after 1100cGy TBI leg bones were digested using collagenase. The cellular fraction of BM and digested bones were pooled together and applied for RNA-seq analysis. For flow cytometry analysis, the flushed BM cell fraction was used for analysis of HSC niche macrophages. The cells collected from bone digestion were used for analyzing osteoprogenitors (OPC), mesenchymal stem cells (MSC) and endothelial cells (EC).

Supplemental Figure 4: Effects of SBDS deficiency on baseline BM osteoprogenitor cells (OPC) and adipogenesis. (A) Unirradiated *Mx1^{Cre}Sbds^{Exc}* mice show no significant baseline reduction in OPC as a percentage of all CD45^{-}TER119^{-} BM stromal cells compared to wildtype (WT) controls. n= 5 mice per group. *p*=0.29, Student's t-test. **(B)** Gene set enrichment analysis (GSEA) plot shows no significant changes of adipogenesis-related gene expression in the BM stromal cells of Mx1^{Cre}SBDS^{Exc} mice versus controls (n=3 mice per group) at baseline. NES: Normalized Enrichment Score. FDR: False Discovery Rate. GSEA statistical test. **(C)** Immunohistochemistry staining indicates a majority of adipocytes present in *Mx1^{Cre}SBDS^{Exc}* BM at 48 hours after 1100cGy TBI are PPAR-γ positive, indicative of recent differentiation. Black arrowheads identify the PPAR-γ-positive nucleus of adipocytes. Scale bar: 50μm.

Supplemental Figure 5: BM niches of irradiated *Mx1^{Cre}SBDS^{Exc}* mice show decreased endothelial cells (EC) and alterations in VEGF signaling. (A) Representative dot plots show the gating strategies and percentages of CD45^{-}TER119^{-}CD31^{+} ECs in CD45^{-}TER119^{-} BM stromal

cells. **(B)** The percentage of ECs in $CD45^{-}TER119^{-}$ BM stromal cells were significantly reduced in $Mx1^{Cre}SBDS^{Exc}$ (n=6) compared to controls (n=5) at 24 hours after 1100cGy TBI. However, no significant change was found at baseline (n=5 mice per group). $^{**}p<0.01$, Student's t-test. **(C)** VEGF-A protein expression by ELISA in BM plasma supernatants harvested from $Mx1^{Cre}SBDS^{Exc}$ and control mice at baseline (n=5 for $Mx1^{Cre}SBDS^{Exc}$ group and n=7 for control group) and 48 hours after 1100 cGy TBI (n=5 for $Mx1^{Cre}SBDS^{Exc}$ group and n=6 for control group). **(D)** GSEA plot showing downregulation of VEGF signaling pathway in the BM stromal cells of $Mx1^{Cre}SBDS^{Exc}$ mice versus controls at 24 hours after TBI (n=5 mice per group), but significant upregulation of VEGF signaling pathway at baseline compared to controls (n=3 mice per group). NES: Normalized Enrichment Score. FDR: False Discovery Rate. **(E)** Changes of expression in individual genes related to VEGF signaling pathway in the BM stromal cells of irradiated (24 hours after 1100cGy TBI) $Mx1^{Cre}SBDS^{Exc}$ mice compared to controls. $^{*}p<0.05$, $^{**}p<0.01$, $^{***}p<0.001$, Student's t-test or *DESeq2* test.

Supplemental Figure 6: SBDS deficiency increases macrophages and decreases phagocytosis in the BM niche after TBI. (A) Representative dot plots show gating strategies for $CD11b^{+}F4/80^{+}Ly6G^{-}$ HSC niche macrophages (MΦ) and $CD11b^{+}F4/80^{-}Ly6G^{+}$ granulocytes within harvested post-TBI BM cells. **(B)** $Mx1^{Cre}SBDS^{Exc}$ mice (n=5) demonstrate higher percentages of $CD11b^{+}F4/80^{+}Ly6G^{-}$ macrophages and lower percentages of $CD11b^{+}F4/80^{-}Ly6G^{+}$ granulocytes in the BM niche than controls (n=7) at 24 hours post-1100 cGy TBI. No significant differences were detected at baseline (n=5 mice per group). *p<0.05, **p<0.01, Student's t-test. **(C)** RNA-seq analysis demonstrating elevated expression of HSC niche macrophage marker genes *Vcam-1*, *Siglec1* (CD169) and *Ackr1* (CD234) in BM stromal cells from irradiated (24 hours after 1100 cGy TBI) $Mx1^{Cre}SBDS^{Exc}$ mice compared to controls. **(D)** GSEA plot demonstrating BM stromal cells of $Mx1^{Cre}SBDS^{Exc}$ mice exhibit downregulation of genes involved in FcγR-mediated phagocytosis at 24 hours post-1100 cGy TBI (n=5 mice per group), but upregulation of these

genes at baseline (n=3 per group). NES: Normalized Enrichment Score. FDR: False Discovery Rate.

Supplemental Figure 7: IGF-1 pathway gene expression in BM niche cells from baseline, unirradiated mice is unaffected by SBDS Deficiency. Gene set enrichment analysis plot showing no significant alterations in IGF-1 signaling pathway gene expression in BM stromal cells from *Mx1^{Cre}SBDS^{Exc}* mice versus controls at baseline. n=3 mice per group. NES: Normalized Enrichment Score. FDR: False Discovery Rate. GSEA statistical test.

Supplemental Figure 8: Effects of SBDS deficiency on BM niche cell activation of p53 signaling, ribosomal protein expression, cell cycle gene expression, and apoptosis at baseline and following TBI. (A) GSEA analysis results show no significant change in genes encoding ribosomal proteins and genes associated with peptide chain elongation in BM stromal cells from *Mx1^{Cre}Sbds^{Exc}* mice versus *Sbds$^{l/l}$* mice at baseline. **(B)** Multiple individual ribosomal genes exhibit a trend towards downregulated niche expression in irradiated (24 hours after 1100cGy TBI) *Mx1^{Cre}Sbds^{Exc}* mice versus control mice. **(C)** qPCR shows no significant difference in expression of the ribosomal genes *Rpl3l* and *Rsl24d1* in BM niche cells from irradiated (24 hours after 1100cGy TBI) *Mx1^{Cre}Sbds^{Exc}* mice (n=3) versus *Sbds$^{l/l}$* control mice (n=4). **(D)** GSEA plot shows no significant change in overall gene expression within p53 pathways in BM niche cells from *Mx1^{Cre}Sbds^{Exc}* mice versus *Sbds$^{l/l}$* mice at baseline (left, n=3 mice per group). Bar plot (right) however does show significant differences in expression of individual p53 target genes, including *Hmox1, Gadd45a*, and *Ptpn14*, in BM niche cells from *Mx1^{Cre}Sbds^{Exc}* mice versus *Sbds$^{l/l}$* mice at baseline. **(E)** GSEA plots indicate overall downregulation of genes related to G1/S cell cycle transition (top) and S-phase DNA synthesis (bottom) in SBDS-deficient BM niche cells compared to controls at baseline (n=3 mice per group). **(F)** GSEA plots show similar downregulation of genes related to G1/S cell cycle transition (top) and S-phase DNA synthesis (bottom) in *Mx1^{Cre}Sbds^{Exc}* versus control *Sbds$^{l/l}$* niche cells at 24 hours after 1100cGy of TBI (n=5

mice per group). **(G)** Immunohistochemical staining for activated Caspase-3, demonstrating increased apoptotic cells (Caspase-3^{+}, brown) as a percentage of total nucleated cells in the BM niche environment of irradiated (48 hours after 1100 cGy of TBI) *Mx1*^{Cre}*Sbds*^{Exc} compared to controls. Black Arrows indicate Caspase-3-positive apoptotic BM stromal cells. Black Arrowheads indicate Caspase-3-negative BM stromal cells. NES: Normalized Enrichment Score. FDR: False Discovery Rate. GSEA statistical test or *DEseq2* statistical test. *p<0.05, ** p<0.01, ***p<0.001.